

Mono lacunary phosphomolybdate supported on MCM-41: synthesis, characterization and solvent free aerobic oxidation of alkenes and alcohols

Nilesh Narkhede, Anjali Patel* and Sukriti Singh

Cite this: *Dalton Trans.*, 2014, **43**, 2512Received 30th August 2013,
Accepted 14th November 2013
DOI: 10.1039/c3dt52395k

www.rsc.org/dalton

A new catalyst comprising monolacunary phosphomolybdate and MCM-41 was synthesized and characterized by different physicochemical techniques. The catalytic activity was evaluated by carrying out solvent free aerobic oxidation of alkenes and alcohols. The catalyst showed 60% conversion of styrene and 28% conversion of benzyl alcohol. The superiority of the present catalytic system lies in obtaining better conversion under solvent free and aerobic conditions.

Introduction

Catalyst development is no longer looked upon simply in terms of optimizing atom and energy efficiencies, but as a clean technology. Different aspects of the overall process design, such as choice of solvent-free/green solvent operation and methods of catalyst separation and waste disposal, must be considered. Oxidation reactions of alkenes and alcohols are some of the most important reactions in organic chemistry.¹ They give a variety of products such as carbonyl compounds, epoxides, diols, and products (aldehydes). The commercial synthesis of such compounds often proceeds *via* oxidation by toxic or hazardous stoichiometric oxidants such as chromates, permanganates and peroxides.² In addition to safety considerations, such technologies are also atom inefficient due to poor selectivity and/or additional separation and waste treatment steps to isolate the product, and therefore economically disadvantageous.

Solid catalysts able to utilise O₂ as the oxidant can circumvent these limitations to afford alternative, continuous aerobic processes, with associated safety, economic, and environmental benefits, and represent an elegant class of atom-efficient molecular transformations. Considering the increasing environmental problems, it is highly desirable to use molecular oxygen in place of traditional corrosive, toxic and expensive oxidants.

In this context, polyoxometalates (POMs), especially phosphomolybdates, have been gaining importance due to their excellent redox properties.³ It is known that phosphomolybdates

are more efficient catalysts among the Keggin series for oxidation reactions. In the case of POMs, the dependence of redox potentials on elemental composition is dictated primarily by the presence or absence of the most oxidizing skeletal or “addenda” atom or early transition metal ions, in the present case, molybdenum. Tuning of these properties of phosphomolybdates can be accomplished at atomic/molecular levels by formation of lacunary species.⁴ The lacunary phosphomolybdate can be formed by the removal of one or more molybdenum–oxygen (Mo–O) octahedral moieties from the saturated Keggin anion framework which increases the anionic charge of the complex.⁴

In the literature there are a few reports focusing on the synthesis of mono lacunary phosphomolybdate; however, not much attention has been devoted to this field due to the known difficulty in isolation, and poor thermal as well as kinetic stability. It was hence a challenging task to stabilize these species onto a suitable support. Our group reported the isolation of the sodium salt of lacunary phosphomolybdate for the first time and successfully stabilized the species onto hydrous zirconia⁵ and alumina⁶ and evaluated its catalytic activity in solvent-free oxidation of styrene and benzyl alcohol.

Thus the prospect of supporting these species on metal oxide supports emerges as an attractive pathway to exploit the catalytic activity and opened the opportunity to create more active and selective catalytic systems. Therefore, as an extension of the previous work, it was thought of interest to use a mesoporous support. In the present paper, for the first time, we report the synthesis and characterization of mono lacunary phosphomolybdate supported on MCM-41 as well as its use as a catalyst for carrying out aerobic oxidation of alkenes and alcohols.

A series of catalysts containing 10–40% of mono lacunary phosphomolybdate (PMo₁₁) and MCM-41 were synthesized.

Polyoxometalate and Catalysis Laboratory, Department of Chemistry, Faculty of Science, The M. S. University of Baroda, Vadodara, 390002, India.
E-mail: aupatel_chem@yahoo.com; Tel: +91-265 2795552

The 30% loaded catalyst was characterized by various thermal, spectral, and surface techniques. The catalytic activity was evaluated for the aerobic oxidation of alkenes and alcohols. Styrene and benzyl alcohol were taken as model substrates. The conditions for maximum conversion as well as selectivity for the desired product were optimized by varying different parameters such as the % loading of catalyst, amount of the catalyst, reaction time, and reaction temperature. A catalytic property for the recycled catalyst was evaluated for the oxidation of styrene and benzyl alcohol under optimized conditions.

Experimental

Materials

All chemicals used were of A.R. grade. Sodium molybdate, anhydrous disodium hydrogen phosphate, acetone, nitric acid, CTAB (cetyltrimethyl ammonium bromide), TEOS (tetraethyl orthosilicate), and sodium hydroxide were obtained from Merck and used as received.

Synthesis of the support

MCM-41 was synthesized by following a method reported by us.⁷ Surfactant (CTAB) was added to a very dilute solution of NaOH with stirring at 60 °C. When the solution became homogeneous, TEOS was added dropwise, and the obtained gel was aged for 2 h. The resulting product was filtered, washed with distilled water, and then dried at room temperature. The obtained material was calcined at 555 °C in air for 5 h and designated as MCM-41.

Synthesis of mono lacunary phosphomolybdate (PMo₁₁)

The mono lacunary phosphomolybdate (Na₇[PMo₁₁O₃₉]:16H₂O) was synthesized using our previously reported method.⁵ Sodium molybdate dihydrate (0.22 mol, 5.32 g) and anhydrous disodium hydrogen phosphate (0.02 mol, 0.28 g) were dissolved in 50–70 mL of conductivity water and heated to 80–90 °C followed by the addition of concentrated nitric acid in order to adjust the pH to 4.3. The volume was then reduced to half by evaporation and the product was separated by liquid–liquid extraction with 50–60 mL of acetone. The extraction was repeated until the acetone extract showed the absence of NO₃[−] ions (ferrous sulfate test). The extracted sodium salt was dried in air. The obtained material was designated as PMo₁₁. Analytical calculated (%): Na, 7.65; Mo, 50.12; P, 1.47; O, 39.52. Found (%): Na, 7.60; Mo, 49.99; P, 1.44; O, 39.92.

Synthesis of the catalyst (anchoring of PMo₁₁ to MCM-41)

A series of catalysts containing 10–40% of PMo₁₁ anchored to MCM-41 were synthesized by the impregnation method. One gram of MCM-41 was impregnated with an aqueous solution of PMo₁₁ (0.1/10–0.4/40 g mL^{−1} of double distilled water) and dried at 100 °C for 10 h. The obtained materials were

designated as (PMo₁₁)₁/MCM-41, (PMo₁₁)₂/MCM-41, (PMo₁₁)₃/MCM-41, and (PMo₁₁)₄/MCM-41, respectively.

Characterization

Elemental analyses were carried out using a JSM 5910 LV combined with an INCA instrument for EDX-SEM. TGA was carried out on the Mettler Toledo Star SW 7.01 up to 600 °C. Adsorption–desorption isotherms of samples were recorded on a Micromeritics ASAP 2010 surface area analyser at −196 °C. Specific surface area was calculated using the BET method from the adsorption–desorption isotherms. FT-IR spectra were obtained by using the KBr wafer on the Perkin Elmer instrument. The Raman spectra were recorded on a FT-Raman Spectrophotometer Model Bruker FRA 106. The ³¹P NMR spectra were recorded at 121.49 MHz using a 7 mm rotor probe with 85% phosphoric acid as an external standard. The spinning rate was 5–7 kHz. Catalyst samples after treatment were kept in a desiccator over P₂O₅ until the NMR measurement. The XRD pattern was obtained by using a PHILIPS PW-1830. The conditions were Cu Kα radiation (1.54 Å) and scanning angle from 0° to 60°. SEM was carried out using a JSM 5610 LV combined with an INCA instrument for EDX-SEM.

Catalytic reaction

The oxidation reaction was carried out in a batch-type reactor operated under atmospheric pressure. In a typical reaction, a measured amount of catalyst (0.227 wt% for styrene and 0.231 wt% for benzyl alcohol) was added to a two-necked flask containing substrates (100 mmol) at 80 °C for styrene and 90 °C for benzyl alcohol. The trace amount of (0.2 mol%) *tert*-butyl hydrogen peroxide (TBHP) was added to the reaction in order to initiate the reaction. The reaction was started by bubbling O₂ into the liquid. The reaction was carried out by varying different parameters such as amount of the catalyst, reaction time and reaction temperature. After completion of the reaction, the catalyst was removed and the products were extracted with dichloromethane and analysed on a gas chromatograph (GC) using an Rtx-5 capillary column. The product was identified by comparison with the authentic samples and finally by gas chromatography-mass spectroscopy (GC-MS).

Leaching test

Heteropoly acids can be quantitatively characterized by the heteropoly blue colour, which is observed when it is reacted with a mild reducing agent such as ascorbic acid. In the present study, this method was used for determining the leaching of PMo₁₁ from the support. Standard samples containing 1–5% of PMo₁₁ in water were prepared. To 10 mL of the above samples, 1 mL of 10% ascorbic acid was added. The mixture was diluted to 25 mL. The resulting solution was scanned at a λ_{max} of 785 cm^{−1} for its absorbance values. A standard calibration curve was obtained by plotting values of absorbance against % concentration. 1 g of supported catalyst with 10 mL water was refluxed for 18 h. Then 1 mL of the supernatant solution was treated with 10% ascorbic acid.

Development of blue colour was not observed, indicating that there was no leaching. The same procedure was repeated with styrene and benzyl alcohol and the filtrate of the reaction mixture after completion of the reaction in order to check the presence of any leached PMo_{11} .

Results and discussion

Catalyst characterization

EDX elemental analysis performed on the catalyst was consistent with theoretical expected values (theoretical: P = 0.33%, Mo = 11.23%; observed: P = 0.37%, Mo = 12.4%).

The TGA of PMo_{11} (Fig. 1) shows the initial weight loss of 16% from 30 to 200 °C. This may be due to the removal of adsorbed water molecules. The final weight loss of 1.8% at around 275 °C indicates the loss of water of crystallisation. The TGA of $(\text{PMo}_{11})_3/\text{MCM-41}$ (Fig. 1) shows that initial weight loss up to 150 °C may be due to the removal of adsorbed water molecules. No significant loss occurs up to 350 °C, which indicates the stability of the catalyst up to 350 °C.

The removal of the Mo–O moiety from the parent 12-molybdophosphoric acid (PMo_{12}) leads to the thermally less stable material PMo_{11} . The thermal stability values of PMo_{11} and supported PMo_{11} are 305 °C and 350 °C respectively, which are comparatively lower than the parent PMo_{12} (430 °C) and the supported PMo_{12} (475 °C).⁸

The decrease in the specific surface area for $(\text{PMo}_{11})_3/\text{MCM-41}$ ($485 \text{ m}^2 \text{ g}^{-1}$) as compared to that of MCM-41 ($659 \text{ m}^2 \text{ g}^{-1}$) is as expected and is the first indication of chemical interaction between available surface oxygen of PMo_{11} and the proton of the silanol group of MCM-41.

The comparison of FT-IR bands of PMo_{12} and PMo_{11} is shown in Table 1. The P–O stretching band (1070 cm^{-1}) for PMo_{12} splits into two new bands 1048 and 999 cm^{-1} in PMo_{11} . This is due to the lowering in the symmetry from Td (PMo_{12}) to Cs (PMo_{11}) around the central heteroatom, phosphorus. The

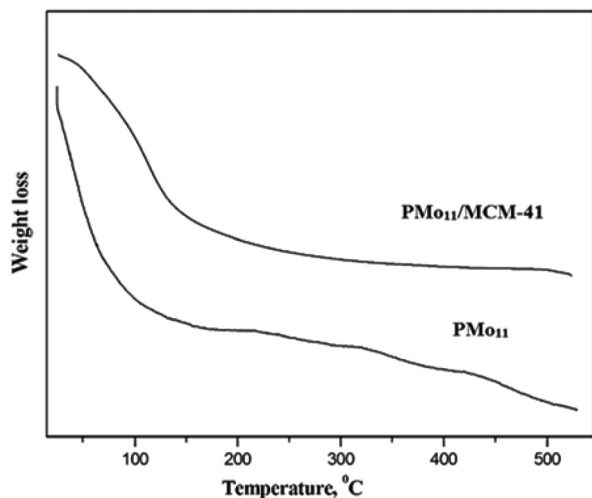


Fig. 1 TGA curves of PMo_{11} and $(\text{PMo}_{11})_3/\text{MCM-41}$.

Table 1 Infrared absorption bands for PMo_{12} and PMo_{11}

POMs	Bands	Wavenumber (cm^{-1})
PMo_{12}	P–O	1070
	Mo=O	965
	Mo–O–Mo	870, 790
PMo_{11}	P–O	1048, 999
	Mo=O	935
	Mo–O–Mo	906, 855

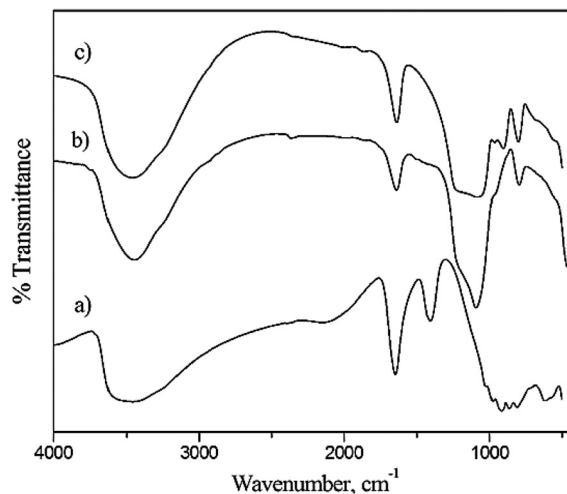


Fig. 2 FT-IR of (a) PMo_{11} , (b) MCM-41 and (c) $(\text{PMo}_{11})_3/\text{MCM-41}$.

presence of these bands confirms the formation of lacunary PMo_{11} .⁹

The FT-IR spectrum of MCM-41 (Fig. 2) shows a broad band around $1300\text{--}1000 \text{ cm}^{-1}$ corresponding to $\nu_{\text{as}}(\text{Si-O-Si})$. The bands at 801 and 458 cm^{-1} are due to symmetric stretching and bending vibration of Si–O–Si, respectively. The band at 966 cm^{-1} corresponds to $\nu_{\text{s}}(\text{Si-OH})$. The FT-IR spectra of PMo_{11} and $(\text{PMo}_{11})_3/\text{MCM-41}$ are presented in Fig. 2. The bands at 1048 and 999 cm^{-1} , 935 and 906 cm^{-1} and 855 cm^{-1} in the parent PMo_{11} are attributed to asymmetric stretches of P–O, Mo=O and Mo–O–Mo, respectively, and are in good agreement with reported values.⁹ The FT-IR of $(\text{PMo}_{11})_3/\text{MCM-41}$ (Fig. 2) shows bands at 965 cm^{-1} and 918 cm^{-1} assigned to P–O and Mo=O stretches, respectively. The shift in the bands is an indication of strong chemical interaction between PMo_{11} and the silanol groups of MCM-41. Further it is confirmed by FT-Raman as well as $^{31}\text{P-NMR}$.

FT-Raman spectra of PMo_{11} and $(\text{PMo}_{11})_3/\text{MCM-41}$ are displayed in Fig. 3. The FT-Raman spectrum of PMo_{11} shows typical bands at 947 ($\nu_{\text{s}}(\text{Mo-O}_d)$), 932 ($\nu_{\text{as}}(\text{Mo-O}_d)$), 891 and 550 ($\nu_{\text{as}}(\text{Mo-O}_b\text{-Mo})$), 355 ($\nu_{\text{as}}(\text{O}_a\text{-P-O}_a)$) and 217 ($\nu_{\text{s}}(\text{Mo-O}_a)$), where O_a , O_b , O_c , and O_d are attributed to the oxygen atoms connected to phosphorus, to oxygen atoms bridging two molybdenums (from two different triads for O_b and from the same triad for O_c), and to the terminal oxygen Mo=O, respectively.⁹ The FT-Raman spectrum of $(\text{PMo}_{11})_3/\text{MCM-41}$ shows the retention of all the characteristic bands at 916 ($\nu_{\text{s}}(\text{Mo-O}_d)$), 876

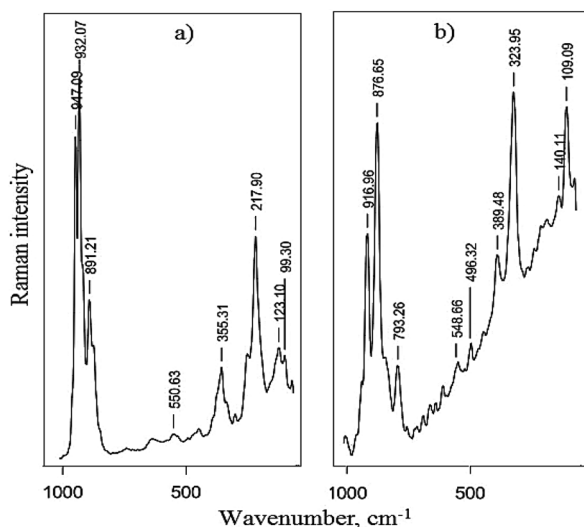


Fig. 3 FT-Raman spectra of (a) PMo_{11} and (b) $(\text{PMo}_{11})_3/\text{MCM-41}$.

($\nu_{\text{as}}(\text{Mo-O}_d)$), 793 and 548 ($\nu_{\text{as}}(\text{Mo-O}_b\text{-Mo})$), 323 ($\nu_{\text{as}}(\text{O}_a\text{-P-O}_a)$) and 140 ($\nu_s(\text{Mo-O}_a)$), which indicates that the structure of PMo_{11} has been retained after anchoring to the support. However, a large shift was observed for all characteristic bands indicating the presence of very strong interaction between the oxygen of PMo_{11} and the hydrogen of the silanol group of MCM-41.

The ^{31}P MAS NMR spectrum of PMo_{11} (Fig. 4) shows a peak at 1.64 ppm corresponding to PMo_{11} . This is in good agreement with the previously reported one.⁵ The catalyst shows a single peak at -1.77 ppm which indicates the presence of undegraded PMo_{11} in the catalyst. The shifting in the peak for the catalyst is due to the interaction of PMo_{11} species with the support. It is reported that the lower shift, *i.e.* deshielding, increases as the degree of adsorption and degree of fragmentation increase.¹⁰ In the present case, the observed chemical shift, shielding, indicates the presence of chemical interaction between PMo_{11} and MCM-41, rather than simple adsorption. Also, a single peak in $(\text{PMo}_{11})_3/\text{MCM-41}$ indicates that no fragmentation of PMo_{11} species takes place after incorporation to the support. Thus it can be concluded that PMo_{11} remains intact inside the channels of MCM-41, as well as the presence

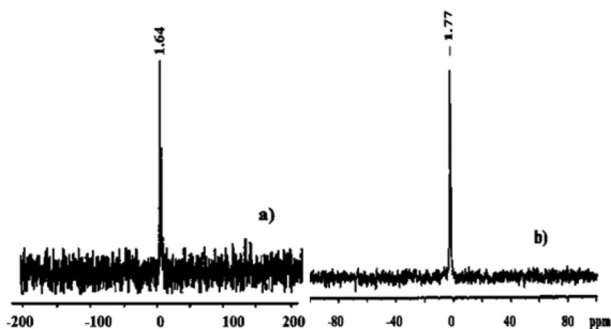


Fig. 4 ^{31}P MAS NMR of (a) PMo_{11} and (b) $(\text{PMo}_{11})_3/\text{MCM-41}$.

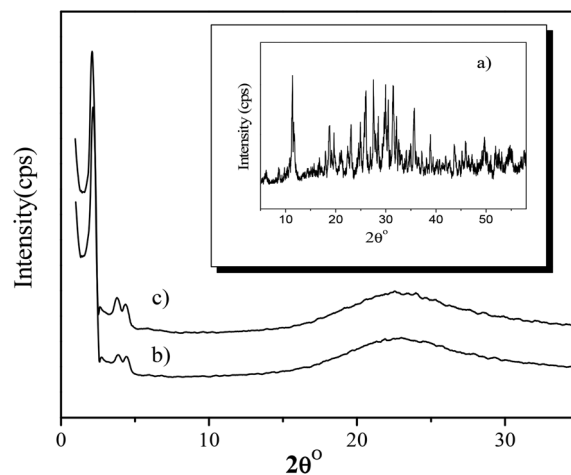


Fig. 5 Powder XRD of (a) PMo_{11} , (b) MCM-41 and (c) $(\text{PMo}_{11})_3/\text{MCM-41}$.

of a chemical interaction between the hydrogen of the surface silanol groups of MCM-41 and PMo_{11} .

The low angle XRD of MCM-41 displays an intense diffraction peak at $2\theta = 2.43^\circ$ and two peaks between $2\theta = 3.2\text{--}4.8^\circ$, which are assigned to the lattice faces (100), (110), and (200), respectively, suggesting a hexagonal symmetry of MCM-41 (Fig. 5). No separate characteristic peak of the crystalline phase of PMo_{11} was observed in $(\text{PMo}_{11})_3/\text{MCM-41}$ which indicates that PMo_{11} is finely dispersed inside the hexagonal channels of MCM-41.

The SEM images of MCM-41 and the catalyst are shown in Fig. 6. The surface morphology of the support is retained in the catalyst. This indicates no aggregates of PMo_{11} on the surface of the catalyst as well as uniform dispersion of PMo_{11} inside the channels of the support.

The FT-IR and ^{31}P MAS NMR shows that PMo_{11} remains intact even after anchoring to the support. BET, FT-IR, FT-Raman and ^{31}P MAS NMR shows that there exists a strong

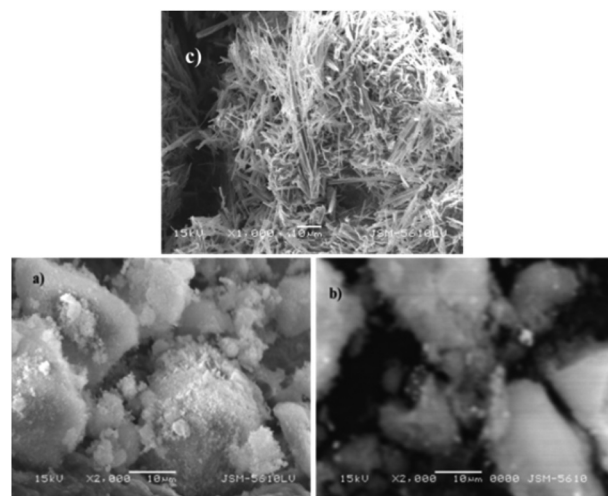


Fig. 6 SEM micrograph of (a) MCM-41, (b) $(\text{PMo}_{11})_3/\text{MCM-41}$ and (c) PMo_{11} .

chemical interaction of PMo_{11} with the support. SEM and XRD results show fine dispersion of PMo_{11} inside the channels of the support.

Catalytic reaction

A detailed catalytic study was carried out on the oxidation of styrene by varying different parameters like % loading, catalyst amount, reaction time and temperature to optimize the conditions for the maximum conversion.

Further in order to check whether the reaction is just auto-oxidation or not, we have carried out control experiments without a catalyst and no conversion of substrates indicates that the reaction does not proceed through auto-oxidation.¹¹

Three different oxidation processes were studied (Table 2), (i) TBHP as the sole oxidant, (ii) using O_2 as the sole oxidant and (iii) employing O_2 as the oxidant with 0.2 mmol TBHP as the initiator. In the case of (i), the reaction did initiate but exclusively polymeric product was obtained for styrene oxidation whereas no conversion was obtained for benzyl alcohol. On comparing the activities of (ii) and (iii) the conversions were almost doubled in the case of (iii) with respect to (ii). This is due to the fact that O_2 as the sole oxidant requires a longer time for activation, *i.e.* a larger induction period, whereas in the case of TBHP as an initiator and O_2 as the main oxidant, TBHP forms species $\text{BuO}^\bullet/\text{OH}$ and hence activates O_2 .

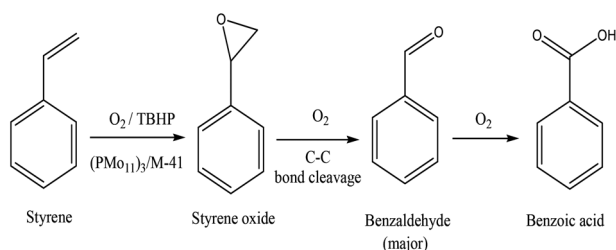
Oxidation of styrene with molecular oxygen

Generally, styrene oxidation gives styrene oxide, benzaldehyde (BA), and benzoic acid (Scheme 1). However, under the present reaction conditions, the major oxidation product obtained was

Table 2 Effect of various oxidants on the epoxidation of styrene

Substrate	Oxidant	% Conversion	Selectivity	
			BA	Others
Styrene ^a	TBHP	44	3	97 ^c
	O_2	39	61	39
	O_2 /TBHP	60	70	30
Benzyl alcohol ^b	TBHP	<1	99	1
	O_2	11	99	1
	O_2 /TBHP	28	90	10

Reaction conditions: reaction temp.: ^a 80 °C, ^b 90 °C, reaction time: ^a 8 h, ^b 24 h, catalyst amount 25 mg, TBHP: 0.2 mmol. ^c Polymer as the major product.



Scheme 1 Aerobic oxidation of styrene.

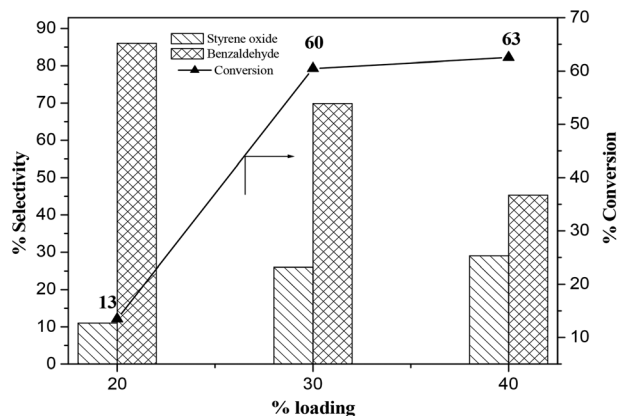


Fig. 7 Effect of % loading on oxidation of styrene. Reaction conditions: 0.2 mmol TBHP; time: 8 h; temperature: 80 °C; amount of catalyst: 0.227 wt%.

benzaldehyde may be because of direct oxidative cleavage of $\text{C}=\text{C}$ of styrene and fast conversion of styrene oxide to BA.

Fig. 7 shows the effect of % loading of PMo_{11} on the oxidation of styrene using molecular oxygen. There is a drastic increase in the conversion of styrene on increasing loading from 20% to 30%. The conversion reaches 60% for 30% loaded catalyst and further increase in the loading to 40% does not affect the conversion significantly. This is because, at higher % loading, the active species agglomerate on the surface of the support resulting in low accessibility to the active sites.

The amount of catalyst has a significant effect on the oxidation of styrene. The oxidation of styrene was carried out by taking catalyst amount in the range 15 mg to 100 mg (Fig. 8). Initially, on increasing catalyst amount from 10 mg to 25 mg, the conversion increases sharply. Further increase in the catalyst amount does not increase the conversion very significantly. Therefore, 25 mg amount of catalyst has been considered as optimum for the maximum conversion.

The effect of reaction time on the selective oxidation of styrene was carried out by monitoring % conversion at

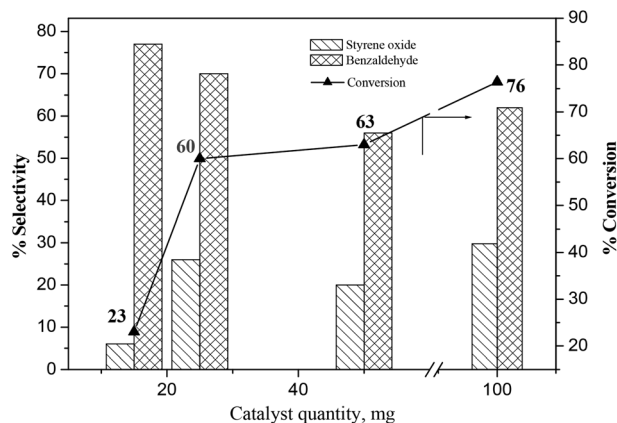


Fig. 8 Effect of catalyst quantity. Reaction conditions: 0.2 mmol TBHP; time = 8 h; temperature = 80 °C.

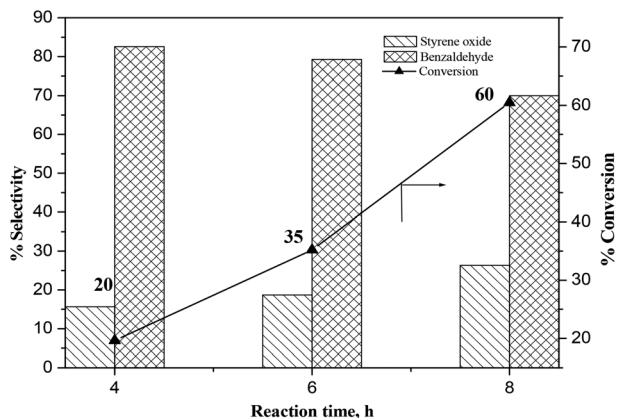


Fig. 9 Effect of reaction time. Reaction conditions: temperature = 80 °C; amount of catalyst: 0.227 wt%; 0.2 mmol TBHP.

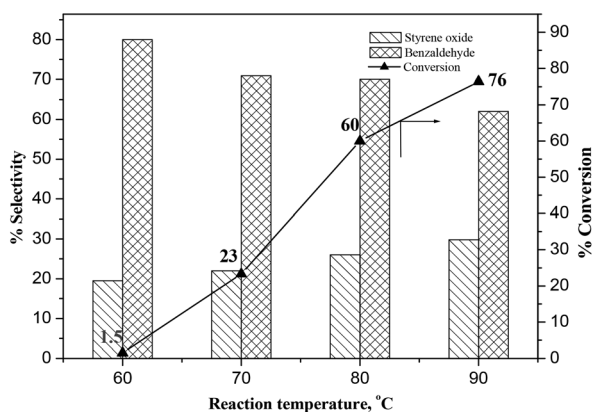


Fig. 10 Effect of reaction temperature. Reaction conditions: 0.2 mmol TBHP; time = 8 h; amount of catalyst: 0.227 wt%.

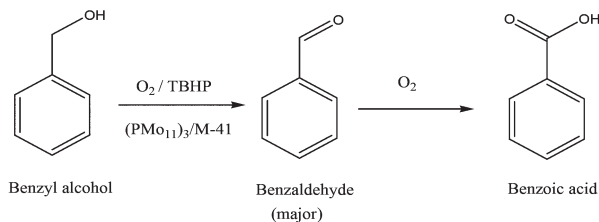
different time intervals. It is seen from Fig. 9 that initially with increase in reaction time up to 6 h, the % conversion increases slowly. The catalyst initially takes an induction period to accelerate the reaction. The maximum conversion was achieved at 8 h of reaction time. On further increase in the reaction time, polymerization starts.

The effect of temperature on the oxidation of styrene was investigated by varying temperature in the range of 60–90 °C (Fig. 10). An optimum of 60% conversion was achieved at 80 °C temperature. When temperature was increased further to 90 °C there is an increase in the conversion but a significant decrease in the selectivity of BA. This is due to over-oxidation of BA to benzoic acid at elevated temperature. Hence, 80 °C was considered as optimum for the maximum conversion as well as selectivity.

The optimum conditions for maximum % conversion (60%) of styrene to benzaldehyde are: loading of PMo_{11} : 30%; catalyst amount: 25 mg (0.227 wt%); time: 8 h; temperature: 80 °C.

Oxidation of benzyl alcohol with molecular oxygen

The catalyst was also explored for the aerobic oxidation of benzyl alcohol. In oxidation of benzyl alcohol, benzaldehyde



Scheme 2 Aerobic oxidation of benzyl alcohol.

(BA) was obtained as a major product along with some amount of benzoic acid as an overoxidation by-product (Scheme 2). The effects of various reaction parameters like % loading, catalyst amount, reaction time and temperature were studied and are shown in Fig. 11.

The optimized conditions for oxidation of benzyl alcohol (28% conversion, 90% selectivity of BA) are as follows: amount of the catalyst – 25 mg (0.231 wt%); time – 24 h and temperature – 90 °C.

Control experiments

The control experiments were carried out using MCM-41 and PMo_{11} for oxidation of styrene and benzyl alcohol under the optimized conditions (Table 3). It is seen from Table 3 that MCM-41 is not much active towards both the reactions, indicating that the catalytic activity is due to PMo_{11} only. The catalytic performance of the catalyst is also presented. The obtained results are almost the same as that of the supported catalyst indicating that PMo_{11} is the real active species.

Heterogeneity and the recycling test

Rigorous evidence of heterogeneity can be gained only by filtering the catalysts before completion of the reaction and analysing the filtrate for activity.¹² A test was performed by filtering the catalyst from the reaction mixture at 90 °C for benzyl alcohol and 80 °C for styrene after a definite period of time, and the filtrate was allowed to react further. The reaction mixture and the filtrate were analysed by a gas chromatogram. No change in the % conversion indicates that the reaction is not just auto-oxidation and the catalyst plays an important role for selective conversion of the substrates. The present catalyst falls into the category C, *i.e.* the active species does not leach and the observed catalysis is truly heterogeneous in nature.¹²

The catalyst was recycled in order to examine its activity as well as stability. The recycling studies were carried out for both the reactions. After the reaction, the catalyst was separated from the reaction mixture by simple centrifugation; the first washing was given with dichloromethane to remove the products, then the subsequent washings were done by double distilled water and then dried at 100 °C, and the recovered catalyst was charged for the further run. No appreciable decrease in the conversion was observed up to two cycles (Table 4). The reused catalyst was further characterized by FT-IR, surface area, FT-Raman and SEM analysis in order to see any structural changes.

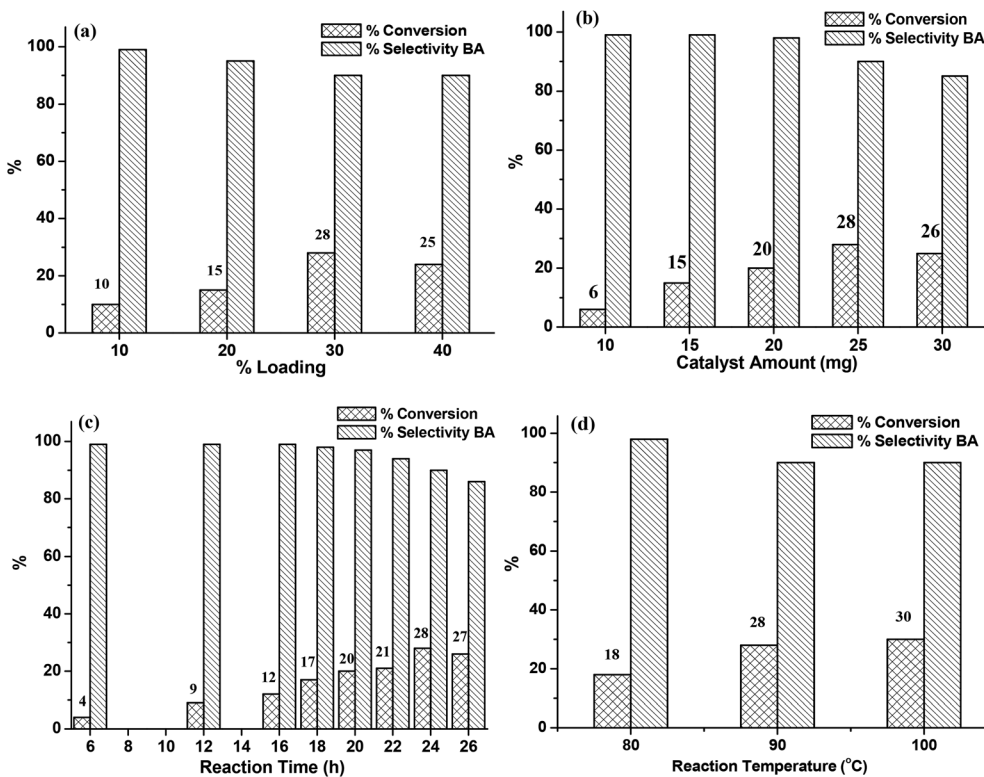


Fig. 11 Optimization of parameters for oxidation of benzyl alcohol: (a) effect of % loading: TBHP (0.2 mmol), amount of catalyst (0.231 wt%), temperature (90 °C), time (24 h); (b) effect of catalyst amount: TBHP (0.2 mmol), temperature (90 °C), time (24 h); (c) TBHP (0.2 mmol), effect of time: amount of catalyst (0.231 wt%), temp. (90 °C); (d) effect of temperature: TBHP (0.2 mmol), amount of catalyst (0.231 wt%), time (24 h).

Table 3 Control experiments over the catalyst and the support

Materials	Substrate	Conversion (%)	Selectivity (%)	
			BA	Styrene oxide
MCM-41	Styrene ^a	<1	>99	—
	Benzyl alcohol ^b	<1	>99	—
PMO ₁₁ ^c	Styrene ^a	43	64	3.8
	Benzyl alcohol ^b	25.2	90.7	—
(PMO ₁₁) ₃ /MCM-41	Styrene ^a	60.0	70.0	26.0
	Benzyl alcohol ^b	28.0	90.0	—

Reaction conditions: 0.2 mmol TBHP, temp.: ^a 80, ^b 90 °C, reaction time: ^a 8 h, ^b 24 h, catalyst amount 25 mg, catalyst amount: ^c 5.7 mg.

Table 4 Recycling studies for both the reactions

Cycle	Conversion (%)	Selectivity (%) BA	TON ^{a/b}
Fresh	60 ^a /28 ^b	70/90	22 472/10 487
1	59 ^a /26 ^b	71/89	22 097/9738
2	55 ^a /25 ^b	68/89	20 599/9363

^a Styrene, ^b benzyl alcohol, O₂: 0.2 mmol TBHP, temp., 80 °C, time, ^a 8 h, ^b 24 h, catalyst amount 25 mg.

Characterization of the recycled catalyst

The FT-IR data for the fresh as well as the regenerated catalyst are presented in Fig. 12a. No appreciable shift in the FT-IR

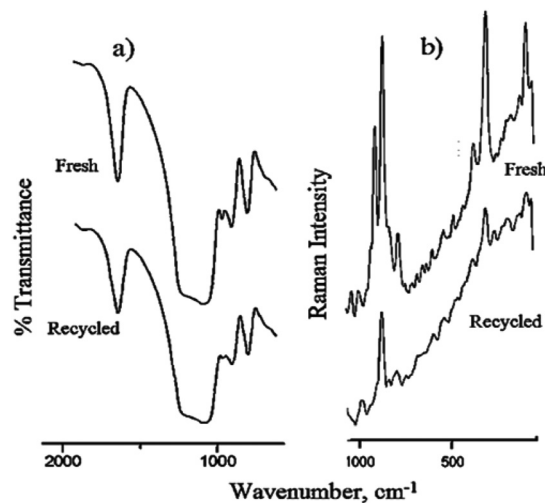


Fig. 12 (a) FT-IR and (b) Raman spectra of fresh and regenerated catalysts.

band position of the regenerated catalyst compared to fresh (PMO₁₁)₃/MCM-41 indicates the retention of structure of PMO₁₁ in the catalyst. This was further confirmed by FT-Raman analysis of the reused catalyst. The Raman spectrum of the spent catalyst (Fig. 12b) shows the retention of the typical bands of PMO₁₁. However, the spectrum is slightly different from the fresh one in terms of intensity.

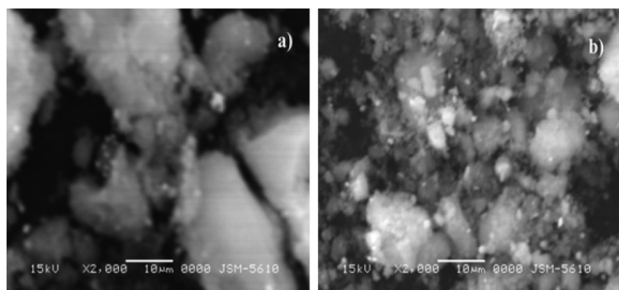


Fig. 13 SEM images of (a) fresh and (b) regenerated catalysts.

Table 5 Oxidation of different substrates by $(\text{PMO}_{11})_3/\text{MCM-41}$

Substrate	Conversion (%)	Products	Selectivity (%)	TON
Styrene ^a	60	BA	70	22 472
α -Methyl styrene ^a	55	Acetophenone	59	20 599
Benzyl alcohol ^b	28	BA	90	10 487
Cyclohexanol ^b	22	Cyclohexanone	>99	8989
Cyclopentanol ^b	20	Cyclopentanone	>99	8240
1-Hexanol ^b	15	1-Hexanal	>99	5618

^a Alkenes, ^b alcohols, O_2 : 0.2 mmol TBHP, temp., ^a 80 °C, ^b 90 °C time, ^a 8 h, ^b 24 h, catalyst amount, 25 mg.

This may be due to the sticking of the substrates on the surface, although this might not be significant in the reutilization of the catalyst.

The SEM images of the fresh and recycled catalyst are shown in Fig. 13. The surface morphology of the catalyst is retained after reusing for several cycles. The above study shows that there is no deactivation of the catalyst after reuse. The BET surface area and pore diameter of the reused catalyst were found to be $470.2 \text{ m}^2 \text{ g}^{-1}$ and 3.68 nm, respectively, which are comparable with the fresh catalyst (surface area: $485 \text{ m}^2 \text{ g}^{-1}$; pore diameter: 3.45 nm).

Oxidation of different alkenes and alcohols

In order to explore the applicability of the method for a selective aerobic oxidation of alkenes and alcohols different substrates were tried (Table 5). In the case of alkenes, styrene and α -methyl styrene produced 70% benzaldehyde and 59% acetophenone, respectively. Employing this system, benzylic, primary and secondary alcohols were oxidized to ketones or aldehydes at 90 °C with moderate to good conversions and excellent selectivities. It was observed from Table 5 that oxidation of secondary alcohol was easier as compared to primary alcohols. The observed trend was in good agreement with a previous report.¹³ It was also observed that the long chain primary alcohol (1-hexanol) is very less reactive under the present reaction conditions. In all the cases we were able to achieve excellent TON for both alkenes and alcohols.

Conclusions

We have synthesized and characterized successfully a new heterogeneous oxidation catalyst comprising PMO_{11} and MCM-41. The BET, FT-IR, and ^{31}P MAS NMR studies show that the structure of PMO_{11} remains intact even after supporting on MCM-41 and there exists a strong chemical interaction with the support. SEM and XRD results show fine dispersion of PMO_{11} inside the channels of the support. We were successful in developing an environmentally benign protocol for selective oxidation of styrene and benzyl alcohol under aerobic conditions using PMO_{11} supported on MCM-41. The applicability of the method was extended to different alkenes and alcohols. In all the cases we found a high TON of >20 500 for alkenes and >5500 for alcohols. The catalyst separation is very simple and can be recovered after simple filtration and is reusable as it retains its catalytic performance. In addition, the advantages of this catalytic system also include good substrate conversion under solvent free reaction conditions and foremost the use of molecular oxygen which make it a greener alternative.

Acknowledgements

We are thankful to the Department of Science and Technology (SR/S5/GC-01/2009) and the University Grants Commission (39-837/2010 (SR)), New Delhi, for the financial support. Ms Sukriti Singh and Mr Nilesh Narkhede are thankful to DST, New Delhi and UGC, New Delhi, respectively, for the award of a research fellowship.

Notes and references

- (a) B. Z. Zhan and A. Thompson, *Tetrahedron*, 2004, **60**, 2917–2935; (b) N. Mizuno, *Modern Heterogeneous Oxidation Catalysis*, Wiley-VCH, 2009; (c) T. Fey, H. Fischer, S. Bachmann, K. Albert and C. Bolm, *J. Org. Chem.*, 2001, **66**, 8154–8159.
- (a) S. L. Regen and C. Koteel, *J. Am. Chem. Soc.*, 1977, **99**, 3837–3838; (b) F. M. Menger and C. Lee, *Tetrahedron Lett.*, 1981, **22**, 1655–1656; (c) C. Wiles, P. Watts and S. J. Haswell, *Tetrahedron Lett.*, 2006, **47**, 5261–5264.
- (a) Y. Ding, B. Ma, Q. Gao, G. Li, L. Yan and J. Suo, *J. Mol. Catal. A: Chem.*, 2005, **230**, 121–128; (b) M. Li, J. Shen, X. Ge and X. Chen, *Appl. Catal., A*, 2001, **206**, 161–169; (c) S. Damyanova, L. Dimitrov, R. Mariscal, J. L. G. Fierro, L. Petrov and I. Sobrados, *Appl. Catal., A*, 2003, **256**, 183–197; (d) G. S. Armatas, G. Bilis and M. Louloudi, *J. Mater. Chem.*, 2011, **21**, 2997–3005.
- (a) C. L. Hill and C. M. P. McCartha, *Coord. Chem. Rev.*, 1995, **143**, 407–455; (b) L. A. C. Walker and Craig L. Hill, *Inorg. Chem.*, 1991, **30**, 4016–4026.
- S. Pathan and A. Patel, *Dalton Trans.*, 2011, **40**, 348–355.

- 6 A. Patel and S. Pathan, *Ind. Eng. Chem. Res.*, 2012, **51**, 732–740.
- 7 V. Brahmkhatri and A. Patel, *Ind. Eng. Chem. Res.*, 2011, **50**, 6620–6628.
- 8 P. Sharma and A. Patel, *Appl. Surf. Sci.*, 2009, **255**, 7635–7641.
- 9 T. Okuhara, N. Mizuno and M. Misono, *Adv. Catal.*, 1996, **41**, 130.
- 10 J. C. Edwards, C. Y. Thiel, B. Benac and J. F. Knifton, *Catal. Lett.*, 1998, **51**, 77–83.
- 11 K. Patel, B. K. Tripuramallu and A. Patel, *Eur. J. Inorg. Chem.*, 2011, **2011**, 1871–1875.
- 12 A. Sheldon, M. Walau, I. W. C. E. Arends and U. Schuchardt, *Acc. Chem. Res.*, 1998, **31**, 485–493.
- 13 E. B. Hergovicha and G. Speier, *J. Mol. Catal. A: Chem.*, 2005, **230**, 79–83.